

Current oscillations in Vanadium Dioxide: evidence for electrically triggered percolation avalanches

Tom Driscoll,^{1, 2, a)} Jack Quinn,² Giwan Seo,³ Yong-Wook Lee,⁴ Hyun-Tak Kim,^{3, 5} David R. Smith,¹ Massimiliano Di Ventra,² and Dimitri N. Basov²

¹⁾ *Center for Metamaterials and Integrated Plasmonics, Pratt School of Engineering, Duke University, Durham, NC, 27708, USA*

²⁾ *Physics Department, University of California, San Diego, La Jolla, California 92093, USA*

³⁾ *School of Advanced Device Technology, University of Science and Technology (UST), Daejeon, 305-350, Korea.*

⁴⁾ *School of Electrical Engineering, Pukyong National University, Busan 608-737, South Korea.*

⁵⁾ *Creative research center of Metal-insulator transition, ETRI, Daejeon 305-700, South Korea.*

(Dated: 25 October 2018)

In this work, we experimentally and theoretically explore voltage controlled oscillations occurring in micro-beams of vanadium dioxide. These oscillations are a result of the reversible insulator to metal phase transition in vanadium dioxide. Examining the structure of the observed oscillations in detail, we propose a modified percolative-avalanche model which allows for voltage-triggering. This model captures the periodicity and waveshape of the oscillations as well as several other key features. Importantly, our modeling shows that while temperature plays a critical role in the vanadium dioxide phase transition, electrically induced heating cannot act as the primary instigator of the oscillations in this configuration. This realization leads us to identify electric field as the most likely candidate for driving the phase transition.

I. INTRODUCTION

Vanadium Dioxide (VO_2) has been a material of prolonged scientific interest, due to the plethora of unusual properties associated with the Insulator to Metal phase Transition (IMT) occurring just above room temperature¹. The large conductivity change ratio, combined with an accessible transition temperature and rich correlated-electron physics²⁻⁴ has made this an attractive compound for many researchers. Much attention has historically revolved around controversy over the driving physics of the phase transition; particularly whether it is a Mott transition⁵⁻⁷ or Pierels transition^{2,8,9}. However, also of interest is the ability of the IMT to happen on ultrafast (100fs) timescales¹⁰, and the wide range of stimuli which can trigger it^{11,12}. Along these lines, recent interest has also shifted from purely academic to industrial as well; following proposed applications ranging from optical devices¹³ and hybrid-metamaterials¹⁴⁻¹⁶ to electronic components^{17,18} and data storage^{19,20}. With this rise of potential applications comes opportunities for new avenues of research and development, but also new challenges to satisfy the durability and flexibility that real-world devices demand²¹. Understanding the role of temperature and structural transitions in various VO_2 phenomenon is key to pushing towards potential of applications.

In this manuscript we take an interest in the recently reported^{22,23} phenomenon of self-sustaining oscillations

in VO_2 bridges. The widespread prevalence of voltage controlled oscillators in electronics makes this phenomenon an enticing candidate for devices. It is fairly well accepted that these oscillations represent a triggering of the Insulator-to-Metal Transition (IMT), followed by a resetting Metal-to-Insulator Transition (MIT). However, despite headway on controlling such oscillations in VO_2 ^{23,24}, there is still debate over whether the underlying driving mechanism is thermal or electrostatic. In literature, VO_2 is most often thermally triggered, and yet these oscillations appear to respond to foremost to applied voltage across the device. The unavoidable presence of joule-heating currents through the 2-terminal device during operation, coupled with the observed sensitivity of the oscillations to device temperature^{21,25}, make for a contentious situation.

In our investigation we first experimentally reproduce the oscillations discovered by the authors of Ref²². The use of a high-performance oscilloscope in our experiment gives us access to very fine time-resolution data which is useful in our modeling. The details and data of our experiment are reported in Section II. Following this, we develop a model which replicates and explains the observed waveshape in terms of electrically-triggered domains. Our model, reported in Section III, describes a network of electrically and/or thermally triggered grains. This model is inspired by several previously proposed models^{26,27}. While these previous models also predict avalanche-like transitions under the right conditions²⁶, our model expands on this framework to track time-dependent effects and allow possibility of a voltage-triggered phase-transition. Alongside voltage triggering, we investigate the role of temperature in the

^{a)} Tom.Driscoll@Duke.edu

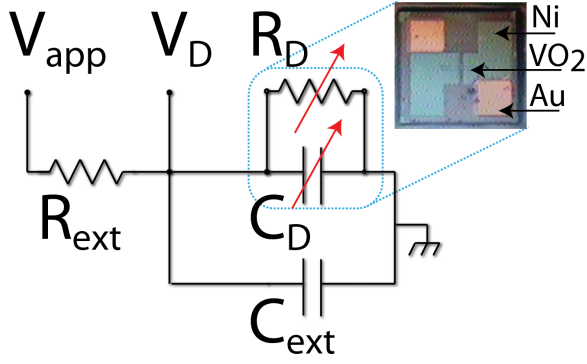


FIG. 1. Schematic of the circuit diagram used to reproduce oscillations, depicting the VO_2 device as a variable resistance and capacitance. Inset shows optical photograph of a sample device. The Al_2O_3 substrate is $330\mu m$ thick, and is mounted on a glass cover slip. All experiments are performed at room temperature.

oscillations, and importantly, we find while a voltage-driven picture replicates experimental data - thermal heating *alone* is quantitatively and qualitatively unable to explain the structure of the observed oscillations. Nevertheless, device temperature does affect oscillations, and thermal co-factors to the voltage triggering are needed to reproduce aspects of the data. In Section IV we discuss how the percolative transition of VO_2 affects the shape of the MIT, and what this means regarding effective medium within the phase-coexistence region. In Section V we conclude the manuscript with an overview of our results, and an outlook on possible directions for VO_2 research and application.

II. VOLTAGE CONTROLLED OSCILLATIONS.

Our investigation begins with replicating VO_2 oscillations using the procedure reported by Kim et.al^{22,24}. A device consisting of a $10\mu m \times 10\mu m$ VO_2 bridge between two large ($\sim 400\mu m$) metal (Ni: Au) electrodes (Figure 1- inset) is hooked in series with a limiting resistor (R_{ext}) and voltage source (V_{app}). This setup is shown schematically in Figure 1. Although we do not intentionally add external capacitance, the presence of such C_{ext} in instruments and cables is unavoidable - and should be included in the effective circuit. The applied voltage V_{app} is a transient square pulse (between $1\mu s$ to $1ms$) from a Agilent function generator (model 33120A) riding on top of a constant bias voltage ($V_{bias} = 12V$). This is shown as the black trace in Figure 2, giving a peak applied voltage of 22V. The voltage across the device (V_D , as shown by the blue trace in Figure 2) is monitored with a LeCroy (model wavepro 7-zi) oscilloscope, which allows for high time-resolution ($40GS/s$) sampling resolution even over millisecond-long pulses.

In this configuration, the VO_2 device functions essentially as a capacitor with a variable internal shunt

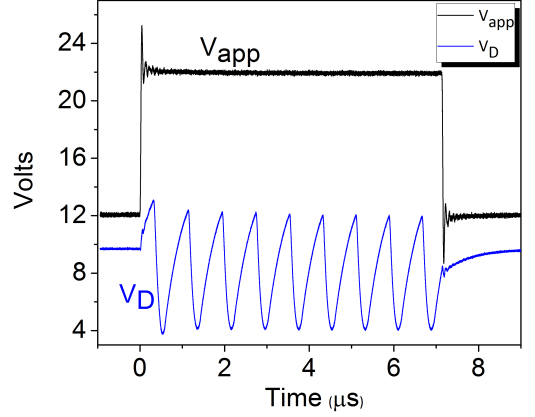


FIG. 2. Applied voltage and voltage across the device as a function of time.

resistance R_D . The capacitance C_D is primarily fixed by device geometry, although variations of the dielectric constant of VO_2 throughout the phase transition (such as have been shown in the context of memory-capacitance^{15,28} and VO_2 hybrid-metamaterials¹⁴) may have small effects - and we discuss this later in Section IV B. The pre-pulse steady-state starting voltage is $V_D = V_{bias} R_D / (R_D + R_{ext})$. At the start of the pulse ($t=0$), V_D increases, following a canonical Resistance-Capacitance (RC) charging curve. Once V_D surpasses a threshold voltage (which we will call $V_{D:IMT}$), it transitions sharply from increasing V_D to decreasing. We assign this change to an IMT event occurring in the VO_2 , which effectively lowers the internal shunt resistance R_D of the capacitor. With lower internal resistance, the capacitor undergoes rapid discharge and V_D plummets. This discharge continues until V_D reaches a lower threshold voltage ($V_{D:MIT}$ at which a second event - which we similarly assign to a Metal-to-Insulator-Transition (MIT) - restores the high internal device resistance. The process reverses and this sequence of events repeats; alternating charging and discharging between IMT and MIT events with a fairly stable periodicity²⁴.

III. GRAIN-SCALE MODEL OF OSCILLATIONS.

Our hope is that by developing a model for these observed oscillations, we may gain insight into the driving mechanism behind them. We start with a 2D network of square VO_2 grains of differing size, each with total resistivity dependent on its size and its state (metal or insulator)^{29,30}. The granularity of polycrystalline VO_2 is well documented^{31,32}, although the size of grains may vary considerably from one VO_2 preparation to another. There is also evidence to suggest the percolation length scales for the IMT may not always coincide with the crystal granularity³³⁻³⁵. A cartoon illustrating our model ar-

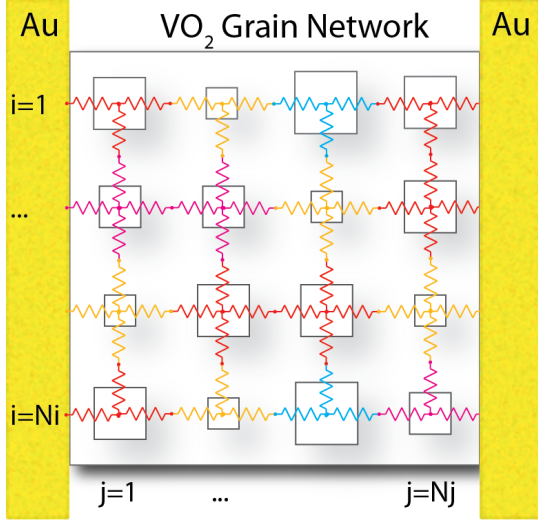


FIG. 3. Cartoon of the grains resistor-network. Left and right sides are the beginning of the nickel electrodes. In the cartoon, the size of squares represent a distribution of grain sizes and resistor colors serve to highlight the corresponding different resistance.

rangement is shown in Figure 3. The network consists of $N_i \times N_j$ grains, and in our model we restrict our investigation to a 50×50 network array to keep computation time manageable.

This grain network is placed in an external circuit containing resistance R_{ext} and capacitance C_{ext} , and driven by V_{app} , as shown in Figure 1. The circuit differential equation (Equation 1), is solved via Runge-Kutta time-stepping.

$$\dot{V}_D(t) = \frac{1}{(C_D + C_{ext})} \left(\frac{V_{app} - V_D}{(R_{ext})} - \frac{V_D}{(R_D)} - \dot{C}_D V_D \right) \quad (1)$$

At each time-step, we solve for the internal state of the grain network. This includes solving a Kirchoff network problem³⁶ for the voltage across each grain and the Thevenin effective circuit resistance R_D . The other VO_2 effective circuit parameter C_D is found by a differential capacitance equation (Equation 2) which can be evaluated via a self-consistent Bruggeman effective medium formulation (Equations 3,4)

$$C_D(t) = C_0 + \eta \frac{\epsilon_D}{\epsilon_0} \quad (2)$$

$$0 = f \frac{\epsilon_m - \epsilon_D}{\epsilon_m + 2\epsilon_D} - (f - 1) \frac{\epsilon_i - \epsilon_D}{\epsilon_i + 2\epsilon_D} \quad (3)$$

$$f = \frac{\sum_{i,j} X^{ij}}{N_i N_j}. \quad (4)$$

Superscript i and j are row and column indices for the grains (running to N_i and N_j total). The binary matrix $X^{ij} = 1$ if the grain i,j is metal and 0 if insulator. η is a capacitive fractional-fields factor (the proportion

of the device capacitance which involves the VO_2 dielectric), which is found via finite element simulation using the COMSOL commercial code package. C_0 is a geometrical capacitance which is determined empirically, fitting $1/RC$ to the capacitive charging curve. External circuit parameters such as R_{ext} and V_{app} are taken directly from experimental values. The extrema values for $R_D(\text{metal})$ and $R_D(\text{insulator})$ are taken from temperature data.

A. Thermal triggering

The temperature driven IMT-MIT has been investigated in great detail and we ground our model using experimental data giving resistance as a function of temperature $R(T)$ through the phase transition. This data is shown in Figure 4a, and displays the characteristic sharp change in resistivity around 345K.

Then, in a procedure similar to previous works^{6,26}, we assume each grain will undergo an IMT in response a "high-threshold" temperature T_{IMT}^{ij} , and a MIT at a low-threshold T_{MIT}^{ij} .

$$R^{ij} = R_{met} \quad \text{if } (T^{ij} > T_{IMT}^{ij}) \quad (5)$$

$$= R_{ins} \quad \text{if } (T^{ij} < T_{MIT}^{ij}) \quad (6)$$

We assign a stochastic distribution to the values of T_{IMT}^{ij} and T_{MIT}^{ij} throughout the network, following the Gaussian form

$$P(T_{IMT}^{ij}) = e^{-\frac{(T_{IMT}^{ij} - T_{0IMT})^2}{2\sigma_{IMT}^2}} \quad (7)$$

$$P(T_{MIT}^{ij}) = e^{-\frac{(T_{MIT}^{ij} - T_{0MIT})^2}{2\sigma_{MIT}^2}}. \quad (8)$$

The values of T_0 and σ^2 are fit to the experimental $R(T)$ data shown in Figure 4a. From this, we find a variance of $T_0 = 340^\circ\text{K}$ and $\sigma_T^2 = 1 \cdot T_0$ reproduces the shape of the IMT fairly well. This fit gives us confidence that we understand the thermal response of VO_2 , even though our thermal model is simple compared to some previous treatments.

Using this temperature-only-triggered model, we attempt to reproduce the oscillations shown in Figure 2. Our model tracks the power dissipated in each grain and employs a finite-element method to solve for the grain and substrate temperatures as a function of time. Material thermal parameters are taken from literature, and the enthalpy of phase-transition for VO_2 is included. Figure 4b re-plots our experimental V_D oscillations in blue, and the model results in green. The result is striking: although we can track V_D for a short while, we are unable to produce any oscillatory phenomena.

Generalizing the behavior that prohibits oscillations, thermal-initiated IMTs exhibit a *runaway* behavior rather than the self-stabilizing oscillatory nature seen in Figure 2. This is apparent in the average VO_2 grain

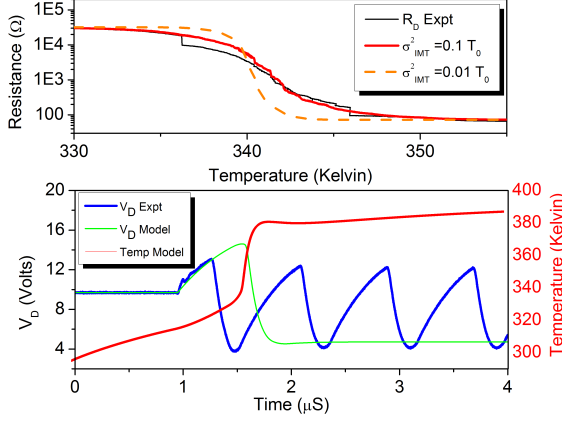


FIG. 4. a) Experimental resistance of our device as a function of temperature $R_D(T)$ (black). $R_D(T)$ results from our model are overlaid for a best-fit value of variance: $\sigma_{IMT}^2 = 0.1 * T_0$ (see Equation 7), which replicates the observed temperature-driven IMT fairly well. Also shown is a poor-fit result for $\sigma_{IMT}^2 = 0.01 * T_0$, given to show the effect of this parameter. b) Attempt to replicate oscillations using thermal-only triggering, with values of $P(T_{IMT}^{ij})$ from above. We plot V_D from our model (green) overlaid on experimental V_D (blue). We observe no oscillations, only a single IMT event. We also plot the average VO_2 temperature T_D from our model, illustrating a runaway heating behavior that precludes oscillations.

temperature plot (red) of 4b. Note that although individual different grains may attain different temperatures over the course of oscillations, such gradients equalize quickly within the network. Average temperature remains a fairly accurate and easily visualized metric of the VO_2 oscillation thermodynamics. As the thermally-triggered IMT occurs, VO_2 temperature skyrockets even while V_D discharges. Once the temperature of the discharged device has surpassed T_{0IMT} , there is no way for it to cool thereafter. Power dissipation and temperature both settle towards steady-state with the device firmly in the metallic state. The causes of this process will become more apparent as we discuss thermal dynamics in Section III D.

B. Electrical triggering

With the failure of a temperature-*only*-triggering model to produce oscillations, and following insights from previous work on voltage-induced effects in VO_2 ,^{22,26,37,38} we now introduce an electric-field driven transition. To do this, we also assign a *voltage drop* at which each grain undergoes phase transition V_{IMT}^{ij} and V_{MIT}^{ij} . We again use random values from a normal dis-

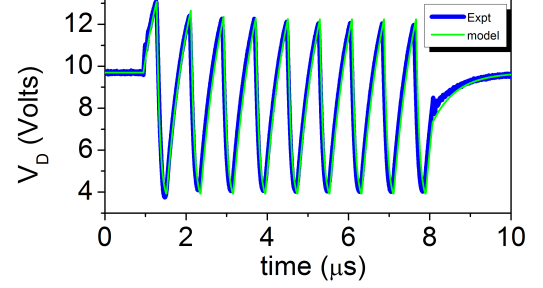


FIG. 5. The experimental data from Figure 2 replotted (blue) with numerical results from our model overlaid (green). This electrical-and-thermal triggering model replicates the experimental data quite well, tracking the oscillation periodicity and producing similar transitions at both $V_{D:IMT}$ and $V_{D:MIT}$.

tribution as we did for T_{IMT}^{ij} and T_{MIT}^{ij} .

$$P(V_{IMT}^{ij}) = e^{-\frac{(V_{IMT}^{ij} - V_{0IMT})^2}{2\sigma_{IMT}^2}} \quad (9)$$

$$P(V_{MIT}^{ij}) = e^{-\frac{(V_{MIT}^{ij} - V_{0MIT})^2}{2\sigma_{MIT}^2}}. \quad (10)$$

We lack direct data to which to fit these distributions (as we did in Figure 4a). Thus, we retain the same value for the variance found in above, $\sigma_V^2 = 0.1 * V_0$. From an energetics perspective, this makes a great deal of sense - both distributions are surely tied to the same underlying Mott-physics. V_0 remains a fitting parameter in our model.

As we have not removed possible thermal triggering, the conditions for grain transition can now be stated as:

$$R^{ij} = R_{met} \quad \text{if}((V^{ij} > V_{IMT}^{ij}) \text{ OR } (T^{ij} > T_{IMT})) \quad (11)$$

$$= R_{ins} \quad \text{if}((V^{ij} < V_{MIT}^{ij}) \text{ AND } (T^{ij} < T_{MIT})) \quad (12)$$

This combined triggering criterion reproduces both the waveshape and periodicity of the experimentally observed oscillations quite well. In Figure 5, we re-plot the experimental data from Figure 2 in blue, and numerical results from our model are shown overlaid in green.

C. Voltage-temperature dependence

Although section III B demonstrated voltage is the primary trigger, device temperature still plays a role in oscillations. There is a known dependence of oscillation amplitude on device temperature²⁵. If we look carefully at the data in Figure 5, we notice a subtle decay envelope to the amplitude of the V_{IMT} oscillation peaks. We believe this envelope is caused by a thermalization of the device on a multi-oscillation timescale. To accommodate

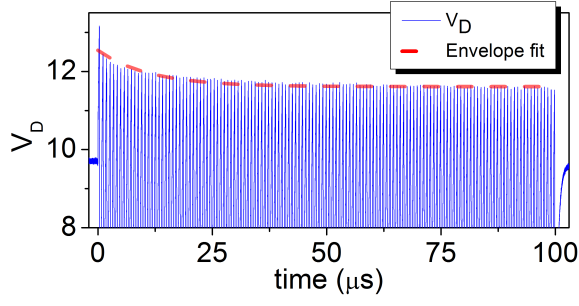


FIG. 6. Experimental data (blue) for oscillations over a long $100\mu\text{s}$ V_{app} pulse. We observe a clear decay envelope to the amplitude of V_{IMT} in the oscillations. For clarity, the bottom half of the oscillations are omitted as we observe no enveloping here. To show this decay is a thermalization envelope caused by device heating, we also plot the temperature dependent $V_{0IMT}(T)$ from equation 13 (red).

this, we include a temperature-dependence to the IMT transition voltage as

$$V_{IMT}^{ij}(T) \rightarrow (\kappa(T - T_0) + 1)V_{IMT}^{ij} \quad (13)$$

where $T_0=295^\circ\text{K}$. κ is a liner temperature coefficient, the fitting of which we discuss below. Without including this voltage-temperature interplay, our model quickly loses sync with the experimental data over the course of several oscillation periods. This thermalization envelope is most clearly observed over a long pluse, and experimental data (solid blue) for a $100\mu\text{s}$ pulse is shown in Figure 6. For clarity in this figure, the bottom half of the oscillations is omitted from view (interestingly, we observe no envelope of V_{MIT}).

Using the data from Figure 6 combined with our thermal-finite element model, we can fit a value for κ . Overlaid on the experimental data (dashed line) is this fit, which gives $\kappa = -8.3 \times 10^{-3}$. This value of κ is used in our oscillation model.

Explanation of this a long time-scale thermalization is straightforward. Although locally the VO_2 film may heat or cool quite quickly in response to current through its volume, the $500\mu\text{m}$ thick sapphire substrate is comparatively massive. The large thermal inertia of the substrate smooths out oscillatory heating away from the film; and when heated only from the top the substrate can require tens of micro-seconds to reach a steady-state temperature gradient.

D. Temperature dynamics

In the above Section III C we have discussed the critical interplay between temperature and voltage-triggering, showing how a long multi-oscillation timescale thermalization envelopes the oscillation amplitude. In this section, we look closer at the temperature evolution on the timescale of the oscillation period.

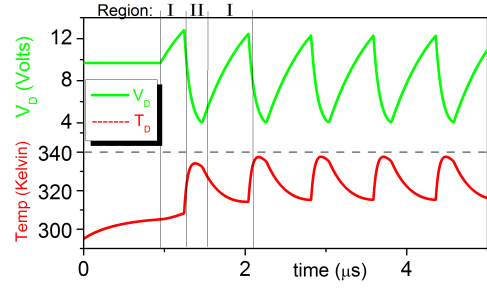


FIG. 7. Model results of temperature dynamics during V_D oscillations. The horizontal dashed line at $T_{IMT}=340^\circ\text{K}$ shows mean transition temperature, and demonstrates that the average temperature reached during oscillations falls short of what's needed to drive the IMT transition. We also divide the oscillation into insulating/charging regions(I) and metallic/discharge regions(II). This draws attention to the sharp *increase* in temperature which occurs only *after* the V_{IMT} trigger, qualitatively discrediting a thermal-driving picture for oscillations.

To begin, in Figure 7 we plot the average grain temperature (red) during oscillations along with V_D (green) - both from our model. Looking at Figure 7 quantitatively, we notice that the average temperature reached is not sufficient to *trigger* oscillations. Although the peak average temperature during the discharge cycle of the oscillation comes close to reaching T_{IMT} , a thermal-driving event would have to occur at-or-before the peak in V_D . The model results indicate that the device is well below T_{IMT} when $V_{D:IMT}$ is reached. The temperature range in Figure 7 agrees fairly well with previous numerical work on the subject³⁹, and our own investigations using commercial finite element package COMSOL. Compared to COMSOL, our home-grown finite-element code over-estimates temperatures reached - perhaps due to difficulty in modeling all of the spatially massive substrate (this is not an issue for commercial packages such as COMSOL). However, commercial codes cannot be run from within Runge-Kutta time-stepping of equation 1, and our code thus critically allows us to calculate temperature dynamics *during* oscillations.

Although a quantitative argument for non-thermal triggering seems compelling, we are acutely aware that precisely solving for temperature can be difficult in such nanoscale systems. Material properties can differ from published bulk values, and interface effects can dominate transport and heating⁴⁰. As we look closely though, the power dissipation in the device also appears *qualitatively* unfit to explain the oscillations. A thermally-driven transition would have to follow the logical sequence:

- I The insulating device heats with applied V_D until it reaches T_{IMT} , where it undergoes an IMT (becoming metallic).
- II The metallic device discharges its stored capacitive energy through the its own volume - cooling as it

discharges - until it reaches T_{MIT} where it undergoes MIT (becoming insulating).

III The process repeats.

However, Figure 7 illustrates that region **II** which occurs after $V_{D:IMT}$ is a region of *maximum* power dissipation; a region of heating not cooling. A simple ohms-law argument explains: Just before and just after the IMT, V_D is approximately $V_{D:IMT}$. However, the resistance R_D has changed by a factor of 10, and thus the power dissipated ($P=V_{D:IMT}^2/R_D$) is substantially greater during region **II** than during region **I**. Thus, we come to the conclusion that a purely-thermal explanation for the oscillations is *qualitatively* as well as quantitatively mismatched to experimental data.

Summarizing Section III, we have identified voltage as a key player in triggering observed oscillations on the grounds of several thermal arguments. One interesting question then is whether electrostatic voltage may also trigger the also IMT in a current-free (ie. FET) configuration. The joule-heating present in our two-terminal device complicates matters, in light of the voltage/temperature interplay identified in Section III C. Previous work has suggested such electrostatic switching can exist,^{6,41,42} although these early results await further confirmation. Exploring the phase-space defined by the interplay of temperature, electrostatic field, and current in these VO_2 oscillations may reveal information about the correlated electron dynamics and energy scales associated with the Mott-transition.

IV. PERCOLATION

In this section, we go into further detail on the mechanisms of the IMT and MIT transitions. Polycrystalline VO_2 is known to exhibit percolative behavior during phase transition^{2,26,34,43}, and this has interesting effects on a voltage-triggered transition. Using the model from Section III which accurately predicts the observed electrical oscillations, we attempt to gain insight on several of the internal processes during oscillatory events.

A. Percolative avalanche driven oscillations

In several previous works^{26,27}, avalanche-like MIT and IMT transitions have been observed under the right conditions. The immediacy of the observed change from charging to discharging in our oscillations leads us to suspect similar avalanche behavior in our electrically-driven device. Examining the details of our model, we see that the voltage drop across any grain in the network (see Figure 3) is proportional to the resistance of the grain. During the charging cycle of the waveform voltage across the entire device (V_D) increases, and V^{ij} across each grain does as well. This charging continues until one "unlucky" grain hits its V_{IMT}^{ij} first. Because the grains receive a

stochastic distribution for V_{IMT}^{ij} (see Equation 9), this can be a random grain anywhere in the network. In experiments, it is seen that the phase-transition is often seeded at particular places such as defects or boundaries.

The unlucky grain that first hits its IMT trigger condition undergoes an IMT. Once this grain becomes metallic, it supports a lower voltage drop ($R_{ins}/R_{met} \approx 20$) - which shifts much of its voltage burden to neighboring grains. The neighboring grains in turn become increasingly likely to undergo their own IMT events. The IMT spreads across the entire sample in an avalanche-like manner. This process is depicted in Figure 8a for a network of 50x50 grains. The upper sequence of black and white frames shows whether each grain is insulating (white) or metallic (black). The lower color frames depict the voltage drop across each grain. The neighbor-neighbor grain interaction, mediated by voltage drop is quite evident.

As is common in percolative systems, the Thevenin resistance R_D of the network is quite sensitive to the spatial distribution of triggered grains. The device resistivity R_D is shown above each frame in the sequence of Figure 8, and we see the largest drop occurs in frames #6 and 7, where the percolation path is completed from left to right. Once a conducting path forms R_D plummets, and V_D begins to drop as the device discharges.

During discharge, there comes a point where V_D drops far enough that a similar process happens in reverse. This MIT is depicted in Figure 8b. However, the MIT process is *not* exactly the reverse of the IMT. The equations governing resistors in parallel tend to "favor" low-resistances in the following manner: Decreasing the value of one resistor (in a parallel network) lowers the Thevenin resistance significantly, but raising the value of a single resistor has only a little effect on the Thevenin resistance. For this reason, the avalanche-like behavior observed in Figure 8a is not seen in Figure 8b. Instead, the process much more closely resembles random percolation, with only moderate neighbor-neighbor interaction. This difference in the mechanisms between IMT and MIT may explain the difference in sharpness of the transitions at $V_{D:IMT}$ and $V_{D:MIT}$ observed in experiments.²⁴

B. Effective medium effects

The percolative nature of the VO_2 phase transition allows for an inhomogeneous intermediate state where both metallic and insulating VO_2 coexist. The dielectric constants of metal and insulating phase VO_2 are distinct; and when both phases can be present in a composite it leads to interesting properties. The average response of the inhomogeneous sample is described by an effective medium, and can have radically different values than either. This leads to quite interesting and novel effects. For example, the inhomogeneity^{2,35} of polycrystalline VO_2 mid-transition is responsible for observed memristance¹⁹ and memory-capacitance^{15,28}.

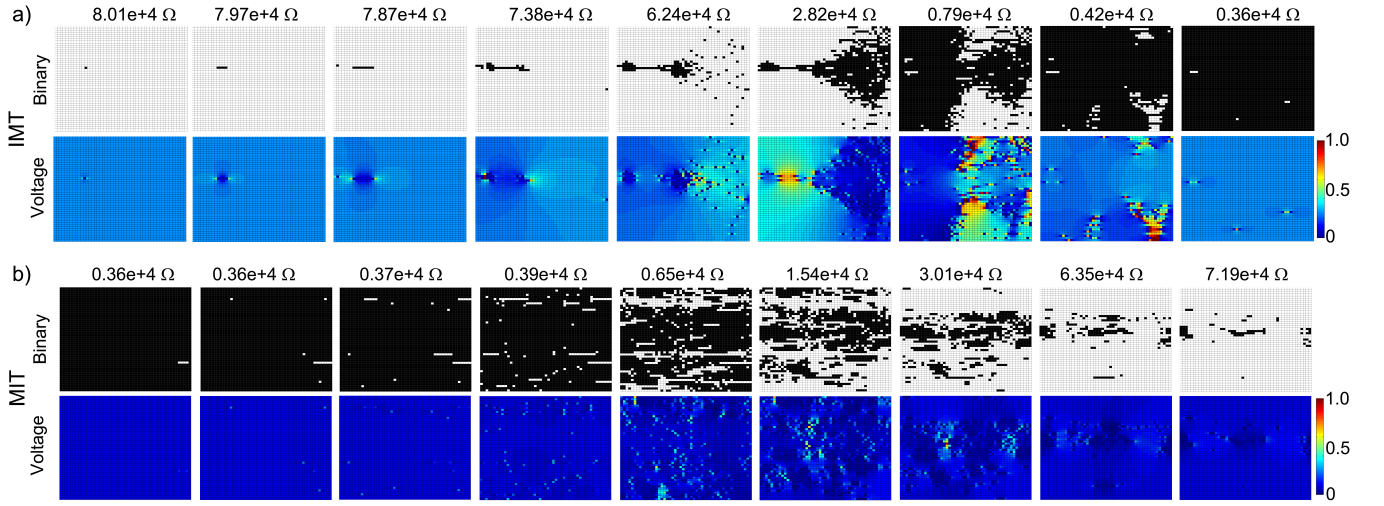


FIG. 8. Step-by-step depiction of the avalanche-like transition for a 50x50 grain network. The time of each frame increases from left to right. a) shows the IMT transition occurring at $V_{D:IMT}$, giving a bi-color plot (top) indicating whether each grain is metallic or insulating and the the voltage (bottom) across each grain in the network. b) shows the same plots for the MIT transition occurring at $V_{D:MIT}$.

The same memory-capacitance as reported in¹⁵ has previously been attributed as playing a key role in voltage-controlled oscillations in VO_2 ²⁴. This is a question we are situated to investigate in more depth using our model. To look closely at the effects of capacitance on the oscillations, we focus attention on a single IMT transition event. In Figure 9, we plot $C_D(t)$ (as calculated from equations 2-4), along with the familiar V_D and R_D .

Looking at Figure 9, as VO_2 transitions from insulating to metallic at the IMT, R_D drops monotonically to its metallic-state value. The capacitance C_D , however, briefly increases before also decreasing to its metallic-state value. This increase is due to the coexistence of metallic and insulating grains, and is predicted by effective medium (Equation 4). However, as Figure 9 shows, the increase in C_D is a small effect, and is contained to a short timespan near the start of the IMT. This leads us to believe the effective medium behavior of C_D has only a minor influence on the shape of the oscillations, and is not a primary driver. We observe the same increase in C_D at the MIT transition edge, but it also is too small and short-lived an effect to bear responsibility for the oscillations.

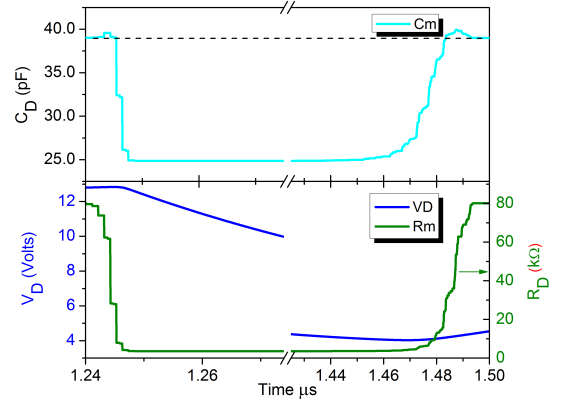


FIG. 9. Model values for C_D plotted with V_D and R_D over one oscillation period. Effective medium within the VO_2 (see Equation 2) causes a brief spike in C_D at immediately near the IMT and MIT transitions. As seen, this spike effect is quite small compared to the overall change of both C_D and R_D , and exists only for a very brief fraction of the oscillation period. The jagged shape of the model curves for R_D and C_D reveal the small jumps typical of percolation discussed in Section IV A

V. SUMMARY

In this work, we have discussed the thermal and electrical driving mechanisms behind observed oscillations occurring in VO_2 films. In addition to experimentally confirming the oscillations reported by Y.W. Lee et.al.²², we have compiled a numerical model which is able to replicate and explain these oscillations in terms of an voltage-triggered Insulator-to-Metal phase-transition. Tempera-

ture is known to trigger the IMT in VO_2 , and temperature plays some role in the shape of the oscillations. However, we find that temperature-only triggering cannot explain oscillations. This result is likely of great importance for applications of these oscillations, as repeated thermal-cycling typically appreciably shortens device lifetime.

One question that remains unaddressed is the role, if any, of the structural phase transition in an electric-field triggered transition. The temperature driven IMT in VO_2 exhibits a structural transition that happens concurrent with the electronic reconfiguration. However, there is evidence^{2,6,34,44–49} to suggest the electronic and structural transitions are not necessarily linked, but merely overlaid. This structural electronic decoupling suggests the electronic correlations in VO_2 play an important role in the IMT phase transition.

Studies which probe the crystal structure simultaneous with these oscillations have not yet been reported - likely because the time and length scales associated with the VO_2 oscillator devices greatly complicate experiments such as x-ray diffraction. However, as mentioned in the introduction (Section I) the question of whether or not the structural transition occurs has great implications about the longevity of these devices. In many applications, devices could easily be expected to perform 10^{12} to 10^{14} oscillation events over their lifetime, a likely impossibility if crystallographic changes are occurring. An evident goal for the near future is to experimentally investigate the existence of structural transition in oscillations in the near future.

VI. ACKNOWLEDGMENTS

T.D. acknowledges support from an IC postdoctoral fellowship. M.D. acknowledges partial support from NSF. This research is supported by AFOSR and ETRI

VII. REFERENCES

- ¹F J Morin. Oxides which show a metal-to-insulator transition at the neel temperature. *Physical Review Letters*, 3(1):34–36, 1959.
- ²Mumtaz M. Qazilbash, Markus Brehm, Byung-Gyu Chae, P.-C. Ho, Gregory O. Andreev, Bong-Jun Kim, Sun Jin Yun, A.V. Balatsky, M.B. Maple, Fritz Keilmann, Hyun-Tak Kim, and Dimitri N. Basov. Mott Transition in VO_2 revealed by Infrared Spectroscopy and Nano-Imaging. *Science*, 318(December):1750–1753, 2007.
- ³Mumtaz M. Qazilbash, AA Schafgans, KS Burch, SJ Yun, BG Chae, BJ Kim, Hyun-Tak Kim, and DN Basov. Electrodynamics of the vanadium oxides VO_2 and V_2O_3 . *Physical Review B*, 77(115121), 2008. doi:10.1103/PhysRevB.77.115121. URL <http://arxiv.org/abs/0803.2739>.
- ⁴M. Liu, B. Pardo, MM Qazilbash, S.J. Yun, BG Chae, BJ Kim, DN Basov, and RD Averitt. Conductivity dynamics in the correlated metallic state of V_2O_3 . In *Lasers and Electro-Optics, 2009 and 2009 Conference on Quantum electronics and Laser Science Conference. CLEO/QELS 2009. Conference on*, volume 4, pages 1–2. IEEE, 2009. URL http://ieeexplore.ieee.org/xpls/abs_all.jsp?arnumber=5225800.
- ⁵A. Zylbersztejn and N.F. Mott. Metal-insulator transition in vanadium dioxide. *Physical Review B*, 11(11):4383, 1975.
- ⁶Hyun-Tak Kim, B G Chae, D H Youn, S L Maeng, G Kim, K Y Kang, and Y S Lim. Mechanism and observation of Mott transition in VO_2 based two- and three-terminal devices. *New Journal of Physics*, 6:52–70, 2004.
- ⁷T.M. Rice, H. Launois, and J.P. Pouget. Comment on "VO₂: Peierls or Mott-Hubbard? A View from Band Theory". *Physical Review Letters*, 73(22):9007–9007, 1994.
- ⁸Renata M Wentzcovitch, Werner W Schulz, and Philip B Allen. VO₂: Peierls or Mott-Hubbard? A View from Band Theory. *Physical Review Letters*, 72(21):3389–3392, 1994.
- ⁹Andrea Cavalleri, Th. Dekorsy, H. Chong, J. Kieffer, and R. Schoenlein. Evidence for a structurally-driven insulator-to-metal transition in VO_2 : A view from the ultrafast timescale. *Physical Review B*, 70(16):3–6, October 2004. ISSN 1098-0121. doi:10.1103/PhysRevB.70.161102. URL <http://link.aps.org/doi/10.1103/PhysRevB.70.161102>.
- ¹⁰Andrea Cavalleri, Cs. Tóth, C W Siders, J A Squier, F Ráksi, P Forget, and J C Kieffer. Femtosecond structural dynamics in VO_2 during an ultrafast solid-solid phase transition. *PRL*, 87:237401:1–4, 2001.
- ¹¹Matteo Rini, Andrea Cavalleri, Robert W Schoenlein, René López, Leonard C Feldman, Richard F Haglund, Lynn A Boatner, and Tony E Haynes. Photoinduced phase transition in VO_2 nanocrystals : control of surface-plasmon resonance ultrafast. *Optics Letters*, 30(5):1–3, 2005.
- ¹²S Lysenko, AJ Rua, V Vikhain, J Jimenez, F Fernandez, and H Liu. Light-induced ultrafast phase transitions in VO_2 thin film. *Applied surface science*, 252(15):5512–5515, 2006. doi:10.1016/j.apsusc.2005.12.137. URL <http://linkinghub.elsevier.com/retrieve/pii/S0169433205018027>.
- ¹³Rene Lopez, L. a. Boatner, T. E. Haynes, R. F. Haglund, and L. C. Feldman. Switchable reflectivity on silicon from a composite $\text{VO}[\text{sub } 2] - \text{SiO}[\text{sub } 2]$ protecting layer. *Applied Physics Letters*, 85(8):1410, 2004. ISSN 00036951. doi:10.1063/1.1784546. URL <http://link.aip.org/link/APPLAB/v85/i8/p1410/s1&Agg=doi>.
- ¹⁴Tom Driscoll, S Palit, Mumtaz M. Qazilbash, Markus Brehm, Fritz Keilmann, Byung-Gyu Chae, Sun-Jin Yun, Hyun-Tak Kim, Nan Marie Jokerst, David R. Smith, and Dimitri N. Basov. Dynamic tuning of an infrared hybrid-metamaterial resonance using vanadium dioxide. *Applied Physics Letters*, 93(024101), 2008. doi:10.1063/1.2956675. URL http://ieeexplore.ieee.org/xpls/abs_all.jsp?arnumber=4838777.
- ¹⁵Tom Driscoll, Hyun-Tak Kim, Byung-Gyu Chae, Bong-Jun Kim, Yong-Wook Lee, Nan Marie Jokerst, S Palit, David R. Smith, Massimiliano Di Ventra, and Dimitri N. Basov. Memory metamaterials. *Science (New York, N.Y.)*, 325(5947):1518–21, September 2009. ISSN 1095-9203. doi:10.1126/science.1176580. URL <http://www.ncbi.nlm.nih.gov/pubmed/19696311>.
- ¹⁶Matthew J Dicken, Koray Aydin, Imogen M Pryce, Luke A Sweatlock, M Boyd, Sameer Walavalkar, James Ma, and Harry A Atwater. Frequency tunable near-infrared metamaterials based on VO_2 phase transition. *Optics Express*, 17(20):295–298, 2009.
- ¹⁷B.J. Kim, Y.W. Lee, B.G. Chae, S.J. Yun, S.Y. Oh, Y.S. Lim, and Hyun-Tak Kim. Temperature dependence of Mott transition in VO_2 and programmable critical temperature sensor. *Arxiv preprint cond-mat/0609033*, 009033v1, 2006. URL <http://arxiv.org/abs/cond-mat/0609033>.
- ¹⁸Tom Driscoll, J. Quinn, S. Klein, Hyun-Tak Kim, B. J. Kim, Yuriy V. Pershin, Massimiliano Di Ventra, and D. N. Basov. Memristive adaptive filters. *Applied Physics Letters*, 97(9):093502, 2010. ISSN 00036951. doi: 10.1063/1.3485060. URL <http://link.aip.org/link/APPLAB/v97/i9/p093502/s1&Agg=doi>.
- ¹⁹Tom Driscoll, Hyun-Tak Kim, B.G. Chae, Massimiliano Di Ventra, and DN Basov. Phase-transition driven memristive system. *Applied Physics Letters*, 95(4):043503, 2009. URL <http://link.aip.org/link/APPLAB/95/043503/1>.

- ²⁰YV Pershin. Memory effects in complex materials and nanoscale systems. *Advances in Physics*, 00(00):1–71, 2011. doi: 10.1080/0001873YYxxxxxxx. URL <http://www.tandfonline.com/doi/abs/10.1080/00018732.2010.544961>.
- ²¹Aurelian Crunteanu, Julien Givernaud, Jonathan Leroy, David Mardivir, Corinne Champeaux, Jean-Christophe Orlianges, Alain Catherinot, and Pierre Blondy. Voltage- and current-activated metalinsulator transition in VO₂-based electrical switches: a lifetime operation analysis. *Science and Technology of Advanced Materials*, 11(6):065002, December 2010. ISSN 1468-6996. doi:10.1088/1468-6996/11/6/065002. URL <http://stacks.iop.org/1468-6996/11/i=6/a=065002?key=crossref.3559a62a92655ee932bf6fc313bbb47a>.
- ²²Y.W. Lee, B.J. Kim, J.W. Lim, S.J. Yun, Sungyul Choi, B.G. Chae, G. Kim, and Hyun-Tak Kim. Metal-insulator transition-induced electrical oscillation in vanadium dioxide thin film. *Applied Physics Letters*, 92(16):162903, 2008. doi: 10.1063/1.2911745. URL <http://link.aip.org/link/APPLAB/92/162903/1>.
- ²³Joe Sakai. High-efficiency voltage oscillation in VO₂ planer-type junctions with infinite negative differential resistance. *Journal of Applied Physics*, 103(10):103708, 2008. ISSN 00218979. doi:10.1063/1.2930959. URL <http://link.aip.org/link/JAPIAU/v103/i10/p103708/s1&Agg=doi>.
- ²⁴Hyun-Tak Kim, Bong-Jun Kim, Sungyul Choi, Byung-Gyu Chae, Yong Wook Lee, Tom Driscoll, Mumtaz M. Qazilbash, and D. N. Basov. Electrical oscillations induced by the metal-insulator transition in VO₂. *Journal of Applied Physics*, 107(2):023702, 2010. ISSN 00218979. doi: 10.1063/1.3275575. URL <http://link.aip.org/link/JAPIAU/v107/i2/p023702/s1&Agg=doi>.
- ²⁵B.J. Kim, Giwan Seo, Y.W. Lee, Sungyul Choi, and Hyun-Tak Kim. Linear Characteristics of a MetalInsulator Transition Voltage and Oscillation Frequency in VO₂ Devices. *Electron Device Letters, IEEE*, 31(11):1314–1316, 2010. URL http://ieeexplore.ieee.org/xpls/abs_all.jsp?arnumber=5595090.
- ²⁶Amos Sharoni, J.G. Ramirez, and I.K. Schuller. Multiple avalanches across the metal-insulator transition of vanadium oxide nanoscaled junctions. *Physical review letters*, 101(2):026404, 2008. doi:10.1103/PhysRevLett.101.026404. URL <http://link.aps.org/doi/10.1103/PhysRevLett.101.026404>.
- ²⁷J.G. Ramirez, Amos Sharoni, Y Dubi, ME Gomez, and I.K. Schuller. First-order reversal curve measurements of the metal-insulator transition in VO₂: Signatures of persistent metallic domains. *Physical Review B*, 79(23):235110, 2009. doi:10.1103/PhysRevB.79.235110. URL <http://prb.aps.org/abstract/PRB/v79/i23/e235110>.
- ²⁸Massimiliano Di Ventra, Yuriy V. Pershin, and Leon O. Chua. Circuit elements with memory: memristors, memcapacitors and meminductors. *Proceedings of the IEEE*, 97(8):1371–1372, January 2009. doi:10.1109/JPROC.2009.2021077. URL <http://arxiv.org/abs/0901.3682>.
- ²⁹John Rozen, Rene Lopez, Richard F. Haglund, and Leonard C. Feldman. Two-dimensional current percolation in nanocrystalline vanadium dioxide films. *Applied Physics Letters*, 88(8):081902, 2006. ISSN 00036951. doi: 10.1063/1.2175490. URL <http://link.aip.org/link/APPLAB/v88/i8/p081902/s1&Agg=doi>.
- ³⁰Jun Dai, Xingzhi Wang, Ying Huang, and Xinjian Yi. Modeling of temperature-dependent resistance in micro- and nanopolycrystalline VO₂ thin films with random resistor networks. *Optical Engineering*, 47(3):033801, 2008. ISSN 00913286. doi: 10.1117/1.2894146. URL <http://link.aip.org/link/OPEGAR/v47/i3/p033801/s1&Agg=doi>.
- ³¹Mei Pan, Hongmei Zhong, Shaowei Wang, Jie Liu, Zhifeng Li, Xiaoshuang Chen, and Wei Lu. Properties of VO₂ thin film prepared with precursor VO (acac)₂. *Journal of Crystal Growth*, 265:121–126, 2004. doi:10.1016/j.jcrysgro.2003.12.065.
- ³²N. R. Mlyuka and R. T. Kivaisi. Correlation between optical, electrical and structural properties of vanadium dioxide thin films. *Journal of Materials Science*, 41(17):5619–5624, June 2006. ISSN 0022-2461. doi:10.1007/s10853-006-0261-y. URL <http://www.springerlink.com/index/10.1007/s10853-006-0261-y>.
- ³³Jecheon Kim, Changhyun Ko, Alex Frenzel, Shriram Ramanathan, and Jennifer E. Hoffman. Nanoscale imaging and control of resistance switching in VO₂ at room temperature. *Applied Physics Letters*, 96(21):213106, 2010. ISSN 00036951. doi:10.1063/1.3435466. URL <http://link.aip.org/link/APPLAB/v96/i21/p213106/s1&Agg=doi>.
- ³⁴Mumtaz M. Qazilbash, a. Tripathi, a. Schafgans, Bong-Jun Kim, Hyun-Tak Kim, Zhonghou Cai, M. Holt, J. Maser, F. Keilmann, O. Shpyrko, and D. Basov. Nanoscale imaging of the electronic and structural transitions in vanadium dioxide. *Physical Review B*, 83(16):1–7, April 2011. ISSN 1098-0121. doi: 10.1103/PhysRevB.83.165108. URL <http://link.aps.org/doi/10.1103/PhysRevB.83.165108>.
- ³⁵Alex. Frenzel, Mumtaz M. Qazilbash, M. Brehm, Byung-Gyu Chae, Bong-Jun Kim, Hyun-Tak Kim, A. Balatsky, F. Keilmann, and D. Basov. Inhomogeneous electronic state near the insulator-to-metal transition in the correlated oxide VO₂. *Physical Review B*, 80(11):1–7, September 2009. ISSN 1098-0121. doi:10.1103/PhysRevB.80.115115. URL <http://link.aps.org/doi/10.1103/PhysRevB.80.115115>.
- ³⁶N. a. Poklonski, a. a. Kocherzhenko, a. I. Benediktovitch, V. V. Mitsianok, and a. M. Zaitsev. Simulation of dc conductance of two-dimensional heterogeneous system: application to carbon wires made by ion irradiation on polycrystalline diamond. *Physica Status Solidi (B)*, 243(6):1212–1218, May 2006. ISSN 0370-1972. doi:10.1002/pssb.200541079. URL <http://doi.wiley.com/10.1002/pssb.200541079>.
- ³⁷Dmitry Ruzmetov, Gokul Gopalakrishnan, Jiangdong Deng, V. Narayanamurti, and Shriram Ramanathan. Electrical triggering of metal-insulator transition in nanoscale vanadium oxide junctions. *Journal of Applied Physics*, 106(8):083702–083702, 2009. doi:10.1063/1.3245338. URL http://ieeexplore.ieee.org/xpls/abs_all.jsp?arnumber=5292009.
- ³⁸G. Stefanovich, A Pergament, and D Stefanovich. Electrical switching and Mott transition in VO₂. *Journal of Physics: Condensed Matter*, 12:8837, 2000. URL <http://iopscience.iop.org/0953-8984/12/41/310>.
- ³⁹Gokul Gopalakrishnan, D. Ruzmetov, and Shriram Ramanathan. On the triggering mechanism for the metalinsulator transition in thin film VO₂ devices: electric field versus thermal effects. *Journal of materials science*, 44(19):5345–5353, 2009. doi: 10.1007/s10853-009-3442-7. URL <http://www.springerlink.com/index/7U24554G53291604.pdf>.
- ⁴⁰Massimiliano Di Ventra. *Electrical transport in nanoscale systems*. Cambridge University Press, Cambridge, 2008.
- ⁴¹Feliks Chudnovskiy, Serge Luryi, and Boris Spivak. Switching device based on first-order metal-insulator transition induced by external electric field. *Future Trends in Microelectronics: the Nano Millennium*, pages 148–155, 2002.
- ⁴²Mumtaz M. Qazilbash, Z. Q. Li, V. Podzorov, M. Brehm, F. Keilmann, B. G. Chae, Hyun-Tak Kim, and D. N. Basov. Electrostatic modification of infrared response in gated structures based on VO₂. *Applied Physics Letters*, 92(24):241906, 2008. ISSN 00036951. doi:10.1063/1.2939434. URL <http://link.aip.org/link/APPLAB/v92/i24/p241906/s1&Agg=doi>.
- ⁴³Tai-Lung Wu, Luisa Whittaker, Sarbajit Banerjee, and G. Sambandamurthy. Temperature and voltage driven tunable metal-insulator transition in individual W_xV_{1-x}O₂ nanowires. *Physical Review B*, 83(7):2–5, February 2011. ISSN 1098-0121. doi: 10.1103/PhysRevB.83.073101. URL <http://link.aps.org/doi/10.1103/PhysRevB.83.073101>.
- ⁴⁴E. Arcangeletti, L. Baldassarre, D. Di Castro, S. Lupi, L. Malavasi, C. Marini, a. Perucchi, and P. Postorino. Evidence of a Pressure-Induced Metallization Process in Monoclinic VO₂. *Physical Review Letters*, 98(19):1–4, May 2007. ISSN 0031-9007. doi:10.1103/PhysRevLett.98.196406. URL

- <http://link.aps.org/doi/10.1103/PhysRevLett.98.196406>.
- ⁴⁵Jiang Wei, Zenghui Wang, Wei Chen, and D.H. Cobden. New aspects of the metalinsulator transition in single-domain vanadium dioxide nanobeams. *Nature Nanotechnology*, 4(7):420–424, 2009. doi:10.1038/NNANO.2009.141. URL <http://www.nature.com/nnano/journal/v4/n7/abs/nnano.2009.141.html>.
- ⁴⁶Tao Yao, Xiaodong Zhang, Zhihu Sun, Shoujie Liu, Yuanyuan Huang, Yi Xie, Changzheng Wu, Xun Yuan, Wenqing Zhang, Ziyu Wu, Guoqiang Pan, Fengchun Hu, Lihui Wu, Qinghua Liu, and Shiqiang Wei. Understanding the Nature of the Kinetic Process in a VO₂ Metal-Insulator Transition. *Physical Review Letters*, 105(22):2–5, November 2010. ISSN 0031-9007. doi: 10.1103/PhysRevLett.105.226405. URL <http://link.aps.org/doi/10.1103/PhysRevLett.105.226405>.
- ⁴⁷Bong-Jun Kim, Yong Wook Lee, Byung-Gyu Chae, Sun Jin Yun, Soo-Young Oh, Hyun-Tak Kim, and Yong-Sik Lim. Temperature dependence of the first-order metal-insulator transition in VO[_{sub} 2] and programmable critical temperature sensor. *Applied Physics Letters*, 90(2):023515, 2007. ISSN 00036951. doi: 10.1063/1.2431456. URL <http://link.aip.org/link/APPLAB/v90/i2/p023515/s1&Agg=doi>.
- ⁴⁸Bong-Jun Kim, Yong Lee, Sungyeoul Choi, Jung-Wook Lim, Sun Yun, Hyun-Tak Kim, Tae-Ju Shin, and Hwa-Sick Yun. Micrometer x-ray diffraction study of VO₂ films: Separation between metal-insulator transition and structural phase transition. *Physical Review B*, 77(23):1–5, June 2008. ISSN 1098-0121. doi: 10.1103/PhysRevB.77.235401. URL <http://link.aps.org/doi/10.1103/PhysRevB.77.235401>.
- ⁴⁹Hyun-Tak Kim, Byung-Gyu Chae, Doo-Hyeb Youn, Gyungock Kim, Kwang-Yong Kang, Seung-Joon Lee, Kwan Kim, and Yong-Sik Lim. Raman study of electric-field-induced first-order metal-insulator transition in VO[_{sub} 2]-based devices. *Applied Physics Letters*, 86(24):242101, 2005. ISSN 00036951. doi: 10.1063/1.1941478. URL <http://link.aip.org/link/APPLAB/v86/i24/p242101/s1&Agg=doi>.